Journal of Luminescence 252 (2022) 119271

Contents lists available at ScienceDirect

Journal of Luminescence

journal homepage: www.elsevier.com/locate/jlumin

Full Length Article

Emission of Tm^{2+} in alkaline-earth fluoride crystals

Evgeny Radzhabov [a,*], Roman Shendrik [a], Vladimir Pankratov [b]

[a] Institute of Geochemistry SB RAS, Favorskii St. 1a, Irkutsk, 664033, Russian Federation
[b] Institute of Solid State Physics, University of Latvia, 8 Kengaraga Iela, LV-1063, Riga, Latvia

ARTICLE INFO

Keywords:
Absorption emission excitation thulium
Alkaline-earth fluorides

ABSTRACT

The luminescence spectra of 4f-4f and 5 d-4f transitions and absorption spectra of 4f-4f transitions of Tm^{2+} ions were studied in crystals of alkaline earth fluorides CaF_2, SrF_2, BaF_2. The 5 d-4f emission of Tm^{2+} ions was detected in the 680–800 nm region with a decay time in the micro-millisecond time interval. The 4f-4f emission is thermally quenched at temperatures of 250, 300, and 350 K in BaF_2, SrF_2, and CaF_2, which correlates with the distance from the excited level to the bottom of the conduction band.

The splitting of the atomic $^2F_{7/2}$, $^2F_{5/2}$ levels of Tm^{2+} by the cubic field decreases linearly with increasing interion distance. The splitting tends to zero at a distance between fluorines of about 4 Å. The positions of the Tm^{2+} bands in alkaline earth fluorides are well described by ab initio quantum chemical calculations.

1. Introduction

Spectroscopy of Tm^{2+} in CaF_2 crystals was first studied in Refs. [1,2] in connection with its possible application as a laser material [3]. The divalent thulium ion has the ground state $4f^{13}$ with atomic levels $^2F_{7/2}$ and $^2F_{5/2}$ split by 1 eV by spin orbit interaction. The splitting of Tm^{2+} energy levels in the CaF_2 cubic field and the level scheme are considered in detail in papers [4,5].

The allowed 4f-5d transitions of Tm^{2+} in halide crystals are located in the region of 200–700 nm. Luminescence is observed for 5 d-4f transitions at 680–800 nm and for 4f-4f transitions at 1.0–1.3 μm for Tm^{2+} ions [6]. Vibronic spectra of 4f-4f transitions in Tm^{2+} ions have been studied and modeled in CaF_2, SrF_2 crystals [7].

Relatively recent studies have shown the promise of using crystals with Tm^{2+} as effective concentrators of solar radiation [8,9], which stimulates new research on Tm^{2+} in halide crystals [10,11].

Our research was motivated by the need for detailed studies of the Tm^{2+} spectra in nonhygroscopic crystals of alkaline earth fluorides as potential laser media and phosphors for solar concentrators.

2. Experimental

Crystals were grown in vacuum in a graphite crucible by the Stockbarger method in the Institute of Geochemistry SB RAS [12]. The graphite crucible contained six cylindrical cavities with a diameter of 10 mm and a length of 80 mm, which made it possible to simultaneously grow six samples with sizes of 10 × 50 mm with different amounts of impurities. A few percentages of CdF_2 were added into the raw materials for purification from oxygen during growth. Cadmium was not found in the grown crystals due to their evaporation at temperatures higher then 1300°C. Earlier, we used closed crucibles to grow MeF_2 (Me = Ca, Sr, Ba) crystals containing cadmium [13].

We have studied the optical spectra of crystals of alkaline earth fluorides CaF_2, SrF_2, BaF_2 with doped with 0.01, 0.1, 0.3, 1 mol% of TmF_3.

When the crystal was grown, thulium entered the crystals of alkaline earth fluorides in the trivalent form. Transfer to the divalent state was carried out by additive staining, heating the crystal in vacuum in calcium vapor at 750–850 °C [14,15]. The change in Tm^{3+} - Tm^{2+} valence was controlled by the appearance of Tm^{2+} 4f-5d absorption bands in the visible wavelength range of 200–700 nm and the appearance of 4f-4f bands transitions in the region of 1000–1200 nm. In parallel, a decrease in the 4f-4f absorption bands of Tm^{3+} was observed in the wavelength range of about 1200 nm ($^3H_6$ - $^3H_5$) and about 1640 nm ($^3H_6$ - $^3H_4$).

Absorption spectra were measured using a Lambda 950 (range 190–3000 nm), and FT801 (range 5000–500 cm^{-1}) spectrophotometers. The emission spectra were measured on a spectrometer with an MDR2 monochromator. Emission was detected by a H6780-04 Hamamatsu photomodule (range 190–900 nm) or by a INGAAS IG17 × 3000T9

---

* Corresponding author.
E-mail address: eradzh@igc.irk.ru (E. Radzhabov).

https://doi.org/10.1016/j.jlumin.2022.119271
Received 13 June 2022; Received in revised form 9 August 2022; Accepted 1 September 2022
Available online 12 September 2022
0022-2313/© 2022 Elsevier B.V. All rights reserved.

photodiode (Laser Components) (range 800–1750 nm). For measurements at low temperatures (6–330 K), a Janis Research cryostat (CCS-100/204) mounted on a spectrophotometer or spectrometer was used. The $MeF_2–Tm^{2+}$ emission was excited by laser radiation at 405 nm (84 mW) or 447 nm (825 mW).

Excitation in the vacuum ultraviolet region and emission spectra were also measured on the photoluminescence endstation FINESTLUMI of the FinEstBeAMS undulator beamline [16] at 1.5 GeV storage ring of MAXIV synchrotron facility (Lund, Sweden).

3. Calculations

The scheme of f-levels of Tm^{2+} ions in fluoride crystals was calculated using the ORCA 5.0.3 software package [17]. Complete active space self-consistent field (CASSCF + NEVPT) calculation was carried out according to the method described in the tutorial [18]. The active space included 13 electrons distributed in the seven 4f-based orbitals. In a recent paper, the applicability of the SARC2 bases for the ab-initio calculation of f-f transitions in free lanthanides Ln^{3+} is shown with good agreement with experimental data [19]. Relativistic effects were considered with the ZORA method. The ZORA-def2-TZVP basis functions for ligands and SARC2-ZORA-QZVP for the thulium ion were used for the calculation.

The TmF_8 (or TmF_8Me_{12}) cluster was surrounded by point charges (near 1000 charges) to simulate the crystal field at the thulium site. The calculation was carried out in three stages [18]. At the first stage, the initial orbitals of the cluster were calculated. At the second stage, the initial orbitals were used and seven thulium f-orbitals were found and rotated in order to fit the active space. The resulting CASSCF orbitals were used in the third step to calculate the 4f Tm^{2+} levels and transitions between them. The calculations were performed with an increasing distance between ligands and point charges.

The calculated orbitals of the f-shell of the free Tm^{2+} ion are split into two states $^2F_{7/2}$ and $^2F_{5/2}$. The calculated distance between $^2F_{7/2}$ and $^2F_{5/2}$ is 8600 cm^{-1} while the experimental value of the level is 8874 cm^{-1} [20].

4. Results

4.1. Excitation spectra

In the excitation spectra of the infrared emission of Tm^{2+} ions, a number of bands is observed in the region of wavelengths less than 220 nm (Fig. 1). There are distinct bands at 197 and 182 nm both in the excitation and absorption spectra (Fig. 1). A band near 197 nm was also observed in the absorption spectra of $SrF_2–Tm^{2+}$, $BaF_2–Tm^{2+}$ crystals [21]. It is assumed that the absorption bands of Tm^{2+} in the region of 360–700 nm are due to the 4f-5d (e_g) transitions, and the bands at 250–350 nm are due to the 4f-5d (t_{2g}) transitions [21]. Perhaps the absorption bands around 170–230 nm are due to transitions from 4f to 6s states. The short wavelength absorption bands at 142 and 157 nm (see Fig. 1) belong to the 4f-5d transitions of Tm^{3+} ions [22]. Dips are observed in the excitation spectra at these wavelengths. It is possible that the dips in the excitation spectra of $CaF_2–Tm$ at about 140 and 160 nm (see Fig. 1) are due to the absorption of trivalent thulium ions remaining in the crystals after additive coloring.

4.2. Absorption spectra

The grown $MeF_2–TmF_3$ crystals were colorless, since the absorption bands of trivalent thulium ions are in the vacuum ultraviolet region of about 150 nm [21,22]. Upon additive coloring, the crystals acquired a color due to the allowed 4f-5d transitions in Tm^{2+} ions in the wavelength range less than 700 nm. The absorption due to forbidden 4f-4f transitions was much weaker, as a result of which the absorption

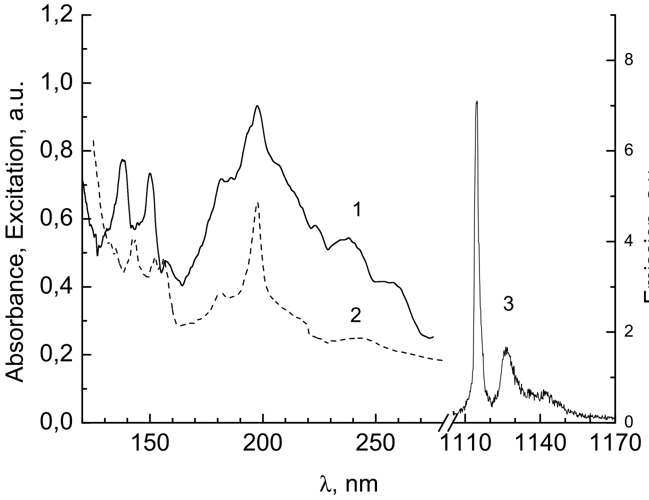

Fig. 1. Excitation (1) and absorption (2) spectra in vacuum ultraviolet and infrared 4f-4f emission spectrum (3) of additively colored $CaF_2–TmF_3$ crystal. Excitation (of 1115 nm emission) and emission (for 151 nm excitation) spectra of CaF_2-0.03 mol% TmF_3 were measured at 10 K. Absorption spectrum of CaF_2-0.01 mol% TmF_3 was measured at 295 K.

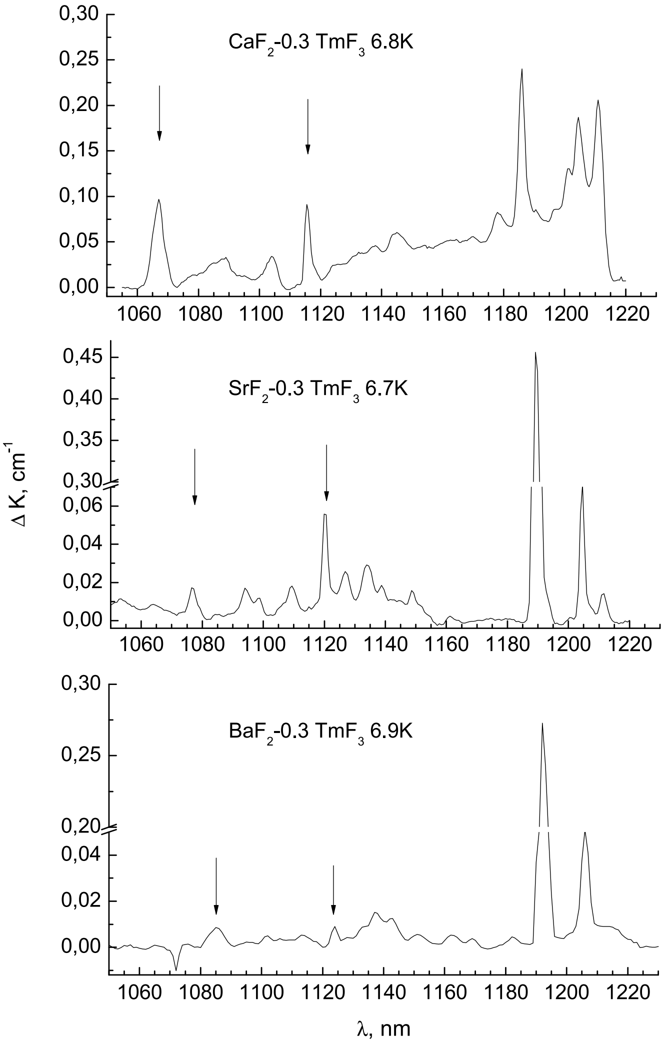

Fig. 2. Absorption spectra of additively colored MeF_2-0.3 mol% TmF_3 crystals. The lines of zero-phonon transitions in Tm^{2+} ions are indicated by arrows. Part of the thulium ions remains in the trivalent state (lines around 1180–1220 nm).

spectra were measured for MeF_2-0.3 mol% TmF_3 crystals (Fig. 2).

In the field of fluorite crystals (O_h symmetry), the Tm^{2+} ground state $^2F_{7/2}$ splits into three components $E_{3/2}$, $E_{1/2}$ and G (or Γ_7, Γ_6, Γ_8) and the excited atomic state $^2F_{5/2}$ splits into two components $E_{3/2}$ and G (or Γ_7', Γ_8') [1,7]. Absorption spectra at low temperatures are due to transitions from the groung state $E_{3/2}$ to states $E_{3/2}$ and G (or Γ_7', Γ_8') accompanied by vibronic bands [7]. In the series of CaF_2–SrF_2–BaF_2 crystals, both lines of zero-phonon transitions are shifted to the long-wavelength side and the distance between them decreases (see Fig. 2). The splitting of atomic levels is caused by the crystal field and obviously should decrease with an increasing lattice constant (see Fig. 2). The shift of the lines of zero-phonon transitions is obviously due to the decrease in the splittings of the ground and excited atomic states (for more details, see the Discussion section).

4.3. Emission spectra

The f-f emission spectra at low temperatures consist of two sharp lines and a vibronic wing towards the long-wavelength side (Fig. 3). The short-wavelength emission line near 1120 nm is due to the Γ_7' - Γ_7 transitions, while the long-wavelength line near 1180 nm arises from the Γ_7' - Γ_8 transitions [1,6]. The rest of the emission bands is caused by the electronic-vibrational interaction [7].

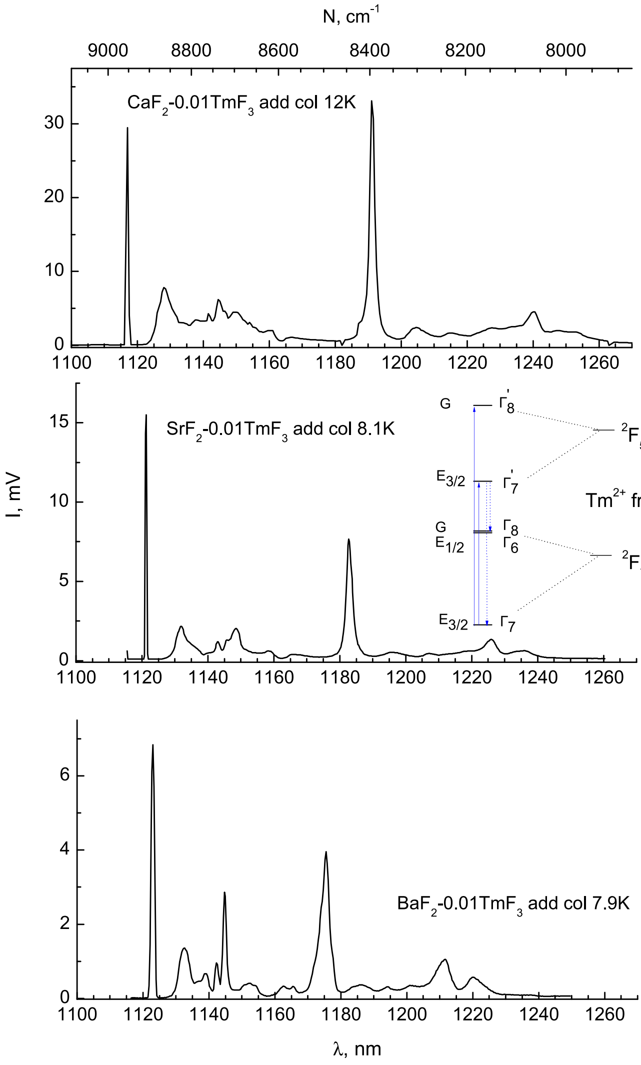

Fig. 3. Luminescence of additively colored MeF_2-0.01 mol% TmF_3 crystals upon excitation by 450 nm laser radiation. The inset shows the scheme of f-levels in MeF_2 crystals adapted from the papers [1,6,23].

When passing from CaF_2 to BaF_2, both emission lines shift towards each other (see Fig. 3). The distance between the lines decreases in the series CaF_2, SrF_2, BaF_2 as 557.8, 464.6, 395.7 cm^{-1}, respectively. With an increase in the interionic distance and a decrease in the strength of the crystal field, the distance between the lines will decrease and, in the limit of an infinite distance, both lines will merge into one with an energy equal to the energy difference between the $^2F_{7/2}$ and $^2F_{5/2}$ Tm^{2+} levels (8774.02 cm^{-1} [20].).

4.4. Temperature dependence

Upon heating, the intensity of f-f lines decreases in two stages and the emission finally disappears around 250, 300, 350 K in BaF_2, SrF_2, CaF_2, respectively (Fig. 4). The first stage of thermal quenching is observed in the range 50–200 K. The reasons for this quenching are not yet clear.

The second stage of quenching is highly dependent on the base cation (see Fig. 4). The quenching activation energy can be considered as the distance from the excited level $^2F_{5/2}$ of the Tm^{2+} ion to the bottom of the conduction band of the crystal. According to the Dorenbos diagrams, these distances are 0.57, 0.87, 0.96 eV for BaF_2, SrF_2, and CaF_2 crystals [24,25]. These energies were estimated from the spectra of optical transitions, while the quenching activation energies obtained by us are due to thermal transitions. Thermal energies are lower than the optical ones, which is caused by the relaxation of the excited state after the optical transition. The thermal quenching energies of 4f-4f Tm^{2+} emission in alkaline earth fluorides are approximately 1.5 times less than the distance from the excited $^2F_{5/2}$ level of the Tm^{2+} ion to the bottom of the conduction band.

4.5. 5 d-4f emission

In the region of 650–780 nm at low temperatures, luminescence bands and lines appear in CaF_2 and BaF_2 crystals, which may be due to 5 d-4f transitions in Tm^{2+} (Fig. 5).

The decay time of the glow at 8 K for both the 710 nm line and the wing (720 nm) is 1.3 μs in CaF_2.

The spectra with a time resolution in the range of 1–2 μs at 10 K and 295 K are in good agreement with the spectra of steady-state luminescence. The emission decay time at 8 K for both the 710 nm line and the wing (720 nm) is 1.3 μs When heated, the decay time decreases at

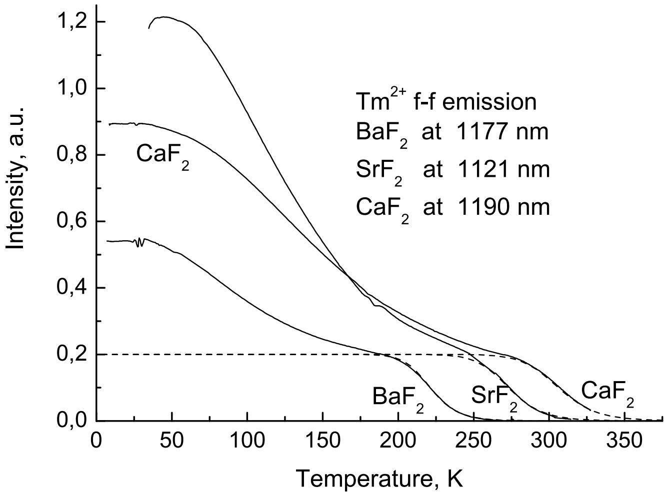

Fig. 4. Temperature dependence of the intensity of 4f-4f radiation of Tm^{2+} in alkaline earth fluorides. The dashed line shows the calculated curves of the temperature dependences of the second stage of Tm^{2+} luminescence in crystals according to the Mott formula with a frequency factor of 5×10^{10} s^{-1} and activation energies of 0.47 (BaF_2), 0.58 (SrF_2), 0.65 eV (CaF_2).

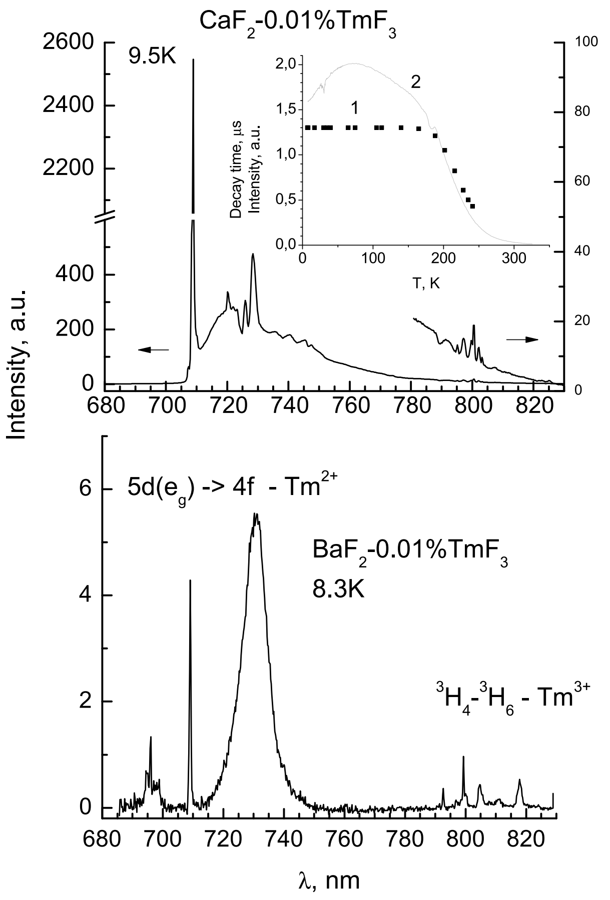

Fig. 5. 5 d-4f emission spectra of Tm^{2+} ions in CaF_2 and BaF_2 crystals upon excitation by 450 nm laser radiation. The lines near 800 nm are due to the emission of Tm^{3+} ions. The inset shows the temperature dependence of decay time (1) and intensity of steady-state luminescence (2) at 720 nm.

temperatures above 170 K. The temperature dependence of the decay time and the intensity of steady-state luminescence above 150 K coincide (see Fig. 5).

In BaF_2, the decay time is substantially less than 0.1 μs When heated, the emission is quenched in the range of 17–80 K.

4.6. Ab-initio calculations

When a Tm^{2+} ion is placed in a crystalline environment, the initially degenerate $^2F_{7/2}$ or $^2F_{5/2}$ levels split in energy. The number of splitting components depends on the symmetry of the crystal field. For a cubic field, the $^2F_{7/2}$ state splits into 3 levels, and the $^2F_{5/2}$ state splits into two levels [23].

The splitting of spin-orbit levels by the crystal field decreases exponentially with increasing distance between the ions. Upon reaching the interionic distance (F–F) equal to 4 Å, the splitting decreases almost to zero.

Since the magnitude of the crystal splitting of the Tm^{2+} levels largely depends on the first sphere of ligands, the geometry of the central Tm–F8 cluster surrounded by a sphere of alkaline earth ions and point charges was optimized. The geometry was optimized using the Gaussian package with the SDD (Tm, F) and LANL2MB (Ca, Sr, Ba) basis sets. It has been established that in CaF2 crystals the distance to the first fluorine sphere increases by 0.1 Å, in SrF_2 crystals it remains unchanged, and in BaF_2 crystals the distance decreases by 0.1 Å. The results obtained reflect the ratio of the crystal radii for coordination 8 of the Tm^{2+}(1.3 Å [26]), Ca^{2+} (1.26 Å), Sr^{2+} (1.4 Å), Ba^{2+} (1.56 Å) [27].

The calculated spin-orbit splitting of Tm^{2+} is only 1.02 times less than the experimental value, but the calculated splitting of the spin-orbit levels by the crystal field shows larger deviation from the experimental values (see Fig. 6).

The calculated positions of the bands are normalized (see Fig. 6) to match the calculated and experimental $^2F_{5/2}$-$^2F_{7/2}$ transitions in free Tm^{2+} thulium ions.

By the geometry optimized distance to the nearest fluorines, the calculated dependence of the crystalline splitting of spin-orbit levels on the lattice parameter is linearized and becomes close to the experimental dependence (see Fig. 6).

5. Discussion

Experimental results show that the integral intensity of the d-f emission decreases significantly in the series CaF_2–SrF_2–BaF_2 (see Fig. 5). This should be expected, since the excited 5 d (e_g) level in these series monotonically approaches the conduction band. According to Dorenbos' model [24,28], the distance 5 d (e_g) of the Tm^{2+} level relative to the bottom of the conduction band is 0.37, 0.1, −0.7 eV in CaF_2–SrF_2–BaF_2, respectively. The excited 5 d (e_g) level in BaF_2 is estimated to be in the conduction band. This is indicated by the low intensity of the luminescence (see Fig. 5) and the rapid decay of the luminescence of Tm^{2+} in BaF_2. It is possible that the relaxation of the excited 5 d (e_g) Tm^{2+} level in BaF_2 shifts it below the bottom of the

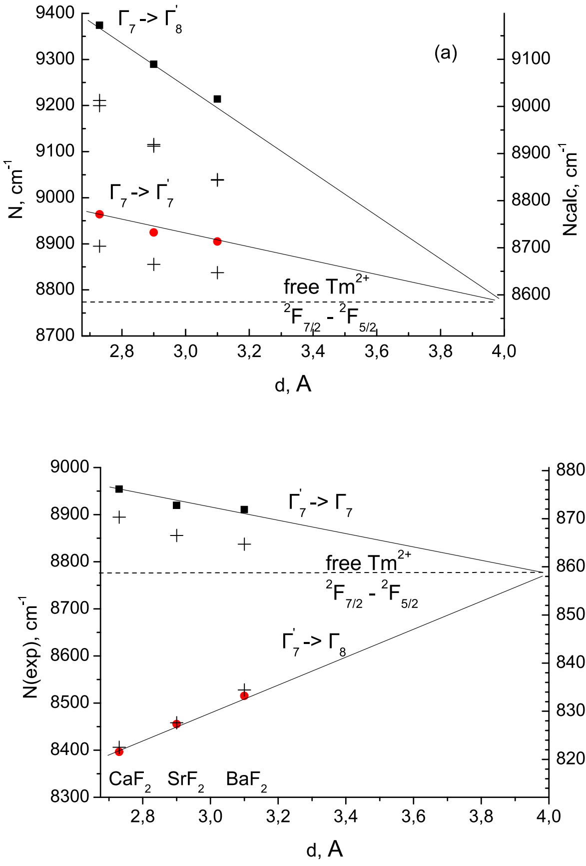

Fig. 6. Position of absorption bands (a), luminescence bands (b) of Tm^{2+} ions in crystals of alkaline earth fluorides. Signs (+) show the ab-initio calculated positions of the bands. The calculated positions of the bands are normalized to match the calculated and experimental $^2F_{5/2}$-$^2F_{7/2}$ transitions in free Tm^{2+} thulium ions.

conduction band, which leads to the appearance of luminescence from this level.

In CaX_2-Tm^{2+} (X = Cl,Br,I) powder phosphors, in addition to the infrared emission band at 1150 nm ($^2F_{5/2}$ - $^2F_{7/2}$), several emission bands were found in the wavelength range 500–1000 nm (5 d t_{2g} - $^2F_{7/2}$) [29]. Visible luminescence bands disappear upon heating in the temperature range 100–250 K with a parallel growth of the infrared band. A coincidence of the temperature dependences of the decay times 5 d t_{2g} - $^2F_{7/2}$ and the rise time $^2F_{5/2}$ - $^2F_{7/2}$ were also found [29]. For the studied fluoride crystals MeF_2 crystals, the 5 d t_{2g} - $^2F_{7/2}$ and $^2F_{5/2}$ - $^2F_{7/2}$ luminescence bands are thermally quenched at temperatures below room temperature, and no phenomena of thermal (through the barrier) energy transfer between the excited levels 5 d and $^2F_{5/2}$.

With an increase in the interionic distance in crystals of alkaline earth fluorides, the energy of the Γ_7-Γ_7' and Γ_7-Γ_8' transitions of Tm^{2+} ions decreases, which is due to a decrease in the crystal splitting of the ground $^2F_{7/2}$ and excited $^2F_{5/2}$ states. The straight lines of both dependences converge at an energy of about 8780 cm^{-1}, which is close to the distance between the $^2F_{7/2}$ and $^2F_{5/2}$ levels in free Tm^{2+} ions (8774.02 cm^{-1} [20]) (Fig. 6a). A different behavior is observed for emission lines (Fig. 6b). With an increase in the lattice constant, the energy of the long-wavelength line Γ_7'-Γ_8 increases, while the energy of the short-wavelength line Γ_7'-Γ_7 decreases. This behavior of the transition energies is consistent with a decrease in the crystalline splitting of states (see Figs. 2 and 3). The straight lines of both dependences also intersect at an energy of about 7800 cm^{-1}, which is close to the energy of the $^2F_{7/2}$-$^2F_{5/2}$ transition in the free Tm^{2+} ion (see Fig. 6). In both cases, the linear dependences intersect at an interion distance of about 4 Å.

In a cubic field, a level with a total moment of 7/2 is split into 3 sublevels according to the Bethe (or Elyashevich) designations Γ_7 ($E_{3/2}$), Γ_8(G), Γ_6 ($E_{1/2}$) and levels with a moment of 5/2 are split into 2 sublevels - Γ_7 ($E_{3/2}$), Γ_8(G) [23]. The zero-phonon transitions in the luminescence spectra are most reliably identified (see Fig. 3). They correspond to transitions to transitions from the lowest excited state Γ_7 ($E_{3/2}$) to the two lower states Γ_7 ($E_{3/2}$), Γ_8(G). The position of the level Γ_6 ($E_{1/2}$) to which the optical transition is forbidden remains undefined. The absorption spectra are much less distinct than the luminescence spectra, but they can also be used to determine zero-phonon transitions (see Fig. 2).

To continue the trend, it would be very interesting to study the optical spectra in CdF_2 crystals with a fluorite lattice and a smaller lattice constant than in CaF_2. In CdF_2 crystals, due to the high second ionization potential of cadmium, the level of the conduction band is strongly shifted down relative to the vacuum level (by 4 eV). The levels of all divalent lanthanides in these crystals, with the exception of Eu^{2+}, fall into the conduction band [30], as a result of which Tm^{2+} ions are not formed.

Ab-initio calculations of the splitting of the $^2F_{7/2}$ or $^2F_{5/2}$ Tm^{2+} levels by crystal field (see Fig. 7) as well as experimental dependences (see Fig. 6) indicate an approximately linear initial decrease in splitting with increasing interionic distance in the range of CaF_2–BaF_2 lattice. With a further increase in the interionic distance, the dependence of the splitting becomes clearly non-linear. The calculated splitting is described by an exponential function, reflecting the radial decrease in the electron density of the thulium and ligands ions.

6. Conclusion

The f-f emission spectra at low temperatures consist of two sharp lines due to transitions from the lowest $^2F_{5/2}$ state to the ground $^2F_{7/2}$ states, split by the crystal field. Upon heating, the f-f emission decreases in two stages and finally disappears at 250, 300, 350 K in BaF_2, SrF_2, CaF_2, respectively. The distance between the emission lines decreases in the series CaF_2, SrF_2, BaF_2 by 240 cm^{-1}, which is associated with a decrease in the strength of the crystal field.

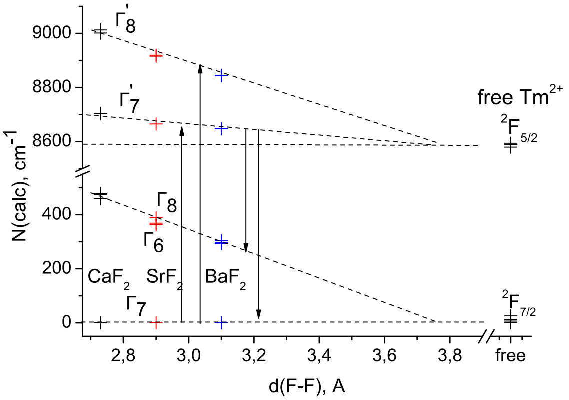

Fig. 7. Ab-initio calculated levels of Tm^{2+} in the crystals field depending on the interionic distance of the lattice. The arrows show the transitions observed in the absorption and luminescence spectra.

In the region of 650–750 nm at low temperatures, all crystals studied exhibit luminescence bands due to 5 d (t_{2g})-4f transitions in Tm^{2+}. The duration of the 5 d-4f emission is in the microsecond range in CaF_2–Tm, BaF_2–Tm and in the millisecond range in SrF_2–Tm.

The relative splitting of the Tm^{2+} atomic states in alkaline-earth fluorides were estimated quite accurately using CASSCF-NEVPT2 ab-initio calculation. The linear decrease in the splitting of the Tm^{2+} levels by the crystal field with an increasing lattice constant is due to the relaxation of the nearest fluorines.

Declaration of competing interest

The authors declare that they have no known competing financial interests or personal relationships that could have appeared to influence the work reported in this paper.

Data availability

No data was used for the research described in the article.

Acknowledgment

The authors gratefully acknowledge V.A. Kozlovskii for preparation of the crystals investigated in this paper.

This study was performed under the project 0284-2021-0004 “Materials and Technologies for the Development of Radiation Detectors, Luminophores, and Optical Glasses” of Russian Academy of Science.

We acknowledge MAX IV Laboratory for time on Beamline FinEstBeams under Proposal 20200308. Research conducted at MAX IV, a Swedish national user facility, is supported by the Swedish Research council under contract 2018–07152, the Swedish Governmental Agency for Innovation Systems under contract 2018–04969, and Formas under contract 2019–02496. Authors are thankful to K. Chernenko for his assistance during experiments at MAX IV.

References

[1] Z.J. Kiss, Energy levels of divalent thulium in CaF_2, Phys. Rev. 127 (3) (1962) 718.

[2] H. Weakliem, Z. Kiss, Zeeman effect of the $^2F_{5/2}$,$E_{5/2}$ - $^2F_{7/2}$,$E_{5/2}$ transition in CaF_2:Tm^{2+}, J. Chem. Phys. 41 (5) (1964) 1507–1508.

[3] R. Duncan Jr., Z. Kiss, Continuously operating CaF_2:Tm^{2+} optical maser, Appl. Phys. Lett. 3 (2) (1963) 23–24.

[4] W. Hayes, P. Smith, Paramagnetic resonance in ground and optically excited states of Tm^{2+} in alkaline earth fluorides, J. Phys. C Solid State Phys. 4 (7) (1971) 840.

[5] B. Bleaney, The spectrum of Tm III in CaF_2, Proc. Roy. Soc. Lond. Math. Phys. Sci. 277 (1370) (1964) 289–296.

[6] J. Grimm, O. Wenger, K. Krämer, H.-U. Güdel, 4f-4f and 4f-5d excited states and luminescence properties of Tm^{2+}-doped CaF_2, $CaCl_2$, $SrCl_2$ and $BaCl_2$, J. Lumin. 126 (2) (2007) 590–596.

[7] I. Ignat'ev, V. Ovsyankin, Electron-vibrational shift of f-levels in CaF_2 and SrF_2 crystals with Tm^{2+} ions, J. Lumin. 72 (1997) 679–680.

[8] K.W. ten Kate, O.M. Krämer, E. van der Kolk, Efficient luminescent solar concentrators based on self-absorption free, Tm^{2+} doped halides, Sol. Energy Mater. Sol. Cell. 140 (2015) 115–120.

[9] E.P. Merkx, M.P. Plokker, E. van der Kolk, The potential of transparent sputtered NaI:Tm^{2+}, $CaBr_2$: Tm^{2+}, and CaI_2: Tm^{2+} thin films as luminescent solar concentrators, Sol. Energy Mater. Sol. Cell. 223 (2021), 110944.

[10] M. Plokker, W. Hoogsteen, R. Abellon, K. Krämer, E. van der Kolk, Concentration and temperature dependent luminescence properties of the SrI_2-TmI_2 system, J. Lumin. 225 (2020), 117327.

[11] N. Chowdhury, N. Riesen, H. Riesen, Photoluminescence of x-ray-induced divalent Tm ions in $BaLiF_3$:Tm^{3+} nanocrystals, J. Phys. Chem. C 125 (39) (2021) 21543–21549.

[12] E. Radzhabov, V. Kozlovsky, Electron transfer between heterogeneous lanthanides in BaF_2 crystals, Radiat. Meas. 122 (2019) 63–66, https://doi.org/10.1016/j.radmeas.2019.01.013.

[13] E. Radzhabov, A. Mysovsky, A. Egranov, A. Nepomnyashikh, T. Kurobori, Cadmium centres in alkaline-earth fluoride crystals, Phys. Status Solidi 2 (1) (2005) 388–391.

[14] E. Radzhabov, A. Egranov, R.Y. Shendrik, Formation of ha-hydrogen centers upon additive coloration of alkaline-earth fluoride crystals, Opt Spectrosc. 122 (6) (2017) 901–905, https://doi.org/10.1134/S0030400X17060182.

[15] E. Radzhabov, Spectroscopy of divalent samarium in alkaline-earth fluorides, Opt. Mater. 85 (2018) 127–132, https://doi.org/10.1016/j.optmat.2018.08.044.

[16] K. Chernenko, A. Kivimäki, R. Pärna, W. Wang, R. Sankari, M. Leandersson, H. Tarawneh, V. Pankratov, M. Kook, E. Kukk, et al., Performance and characterization of the finestbeams beamline at the max iv laboratory, J. Synchrotron Radiat. 28 (5).

[17] F. Neese, F. Wennmohs, U. Becker, C. Riplinger, The ORCA quantum chemistry program package, J. Chem. Phys. 152 (22) (2020), 224108.

[18] D. Aravena, M. Atanasov, V. Chilkuri, Y. Guo, J. Jung, D. Maganas, B. Mondal, I. Schapiro, K. Sivalingam, S. Ye, et al., CASSCF Calculations in ORCA (4.2): A Tutorial Introduction, Available at the following: https://orcaforum.kofo.mpg.de/app.php/dlext/?cat=4.

[19] D. Aravena, F. Neese, D.A. Pantazis, Improved segmented all-electron relativistically contracted basis sets for the lanthanides, J. Chem. Theor. Comput. 12 (3) (2016) 1148–1156.

[20] W. Martin, R. Zalubas, L. Hagan, Atomic Energy Levels-The Rare Earth elements. (The Spectra of Lanthanum, Cerium, Praseodymium, Neodymium, Promethium, Samarium, Europium, Gadolinium, Terbium, Dysprosium, Holmium, Erbium, Thulium, Ytterbium, and lutetium).[66 Atoms and Ions], Tech. rep., Manchester Coll. Of Science and Technology, Dept. of Chemistry, (UK), 1978.

[21] E. Loh, $4f^n$ - $4f^{n-1}5d$ spectra of rare-earth ions in crystals, Phys. Rev. 175 (2) (1968) 533.

[22] M. Schlesinger, T. Szczurek, M. Wade, G. Drake, Anomalies in the vacuum uv absorption spectrum of Yb^{3+} in CaF_2, Phys. Rev. B 18 (11) (1978) 6388.

[23] M. Elyashevich, Spectra of Rare Earth (Gosttekhteorizdat, Moscow, 1953); See Also the Translation Useac, AEC-Tr-4403, Office of Technical Information, Department of Commerce, Washington DC.

[24] P. Dorenbos, Ce^{3+} 5d-centroid shift and vacuum referred 4f-electron binding energies of all lanthanide impurities in 150 different compounds, J. Lumin. 135 (2013) 93–104.

[25] P. Dorenbos, The nephelauxetic effect on the electron binding energy in the 4fq ground state of lanthanides in compounds, J. Lumin. 214 (2019), 116536.

[26] Y. Jia, Crystal radii and effective ionic radii of the rare earth ions, J. Solid State Chem. 95 (1) (1991) 184–187.

[27] R.D. Shannon, Revised effective ionic radii and systematic studies of interatomic distances in halides and chalcogenides, Acta Crystallogr. Sect. A Cryst. Phys. Diffr. Theor. Gen. Crystallogr. 32 (5) (1976) 751–767.

[28] P. Dorenbos, Improved parameters for the lanthanide $4f^q$ and $4f^{q-1}5d$ curves in hrbe and vrbe schemes that takes the nephelauxetic effect into account, J. Lumin. 222 (2020), 117164.

[29] M. Plokker, I. van der Knijff, A. de Wit, B. Voet, T. Woudstra, V. Khanin, P. Dorenbos, E. van der Kolk, Experimental and numerical analysis of Tm^{2+} excited-states dynamics and luminescence in CaX_2 (X=Cl, Br, I), J. Phys. Condens. Matter 33 (25) (2021), 255701.

[30] P. Rodnyi, I. Khodyuk, G. Stryganyuk, Location of the energy levels of the rare-earth ions in BaF_2 and CdF_2, Phys. Solid State 50 (9) (2008) 1639–1643.